Hindawi
Advances in Materials Science and Engineering
Volume 2018, Article ID 3795798, 11 pages
https://doi.org/10.1155/2018/3795798

Research Article

Shot Peening Effects on Subsurface Layer Properties and Fatigue Performance of Case-Hardened 18CrNiMo7-6 Steel

H. S. Ho, D. L. Li, E. L. Zhang, and P. H. Niu

School of Mechanical Engineering and Henan Key Engineering Laboratory of Anti-Fatigue Manufacturing Technology, Zhengzhou University, Science Road 100, Zhengzhou 450001, China

Correspondence should be addressed to E. L. Zhang; erliang.zhang@zzu.edu.cn

Received 13 December 2017; Revised 9 February 2018; Accepted 19 February 2018; Published 17 April 2018

Academic Editor: Zhiping Luo

The present study is conducted with a dual-aim: firstly, to examine the effect of several single shot peening conditions on the subsurface layer properties and fatigue performance of the case-hardened 18CrNiMo7-6 steel, and secondly, to propose an optimized peening condition for improved fatigue performance. By carrying out the subsurface integrity analysis and fatigue testing, the underlying relationships among the peening process, subsurface layer property and fatigue performance are investigated, the way peening conditions affect the fatigue life and its associated scatter for the case-hardened 18CrNiMo7-6 steel is quantitatively assessed. The in-depth study shows that dual peening can be an optimized solution, for it is able to produce a subsurface layer with enhanced properties and eventually gain a significant improvement in fatigue performance.

1. Introduction

High-strength steels are massively used in the aeronautical and automotive applications for their high-loading capacity. With the increasing demand for high reliability products, the dual properties of high strength and high ductility are expected for such steel materials to give a longer service lifetime of engineering machinery. This motivates the design of a new class of material, referred to as gradient nanostructured (GNS) high-strength steel [1]. As fatigue failures generally occur on the material surface and propagate into the interior, a structural architecture comprising a GNS subsurface region and a coarse-grained interior are considered optimal for enhanced fatigue behavior. Loosely speaking, this is because fatigue crack initiation would be suppressed by the strong work-hardened subsurface layer of a fine-grained structure, and fatigue crack propagation would be arrested by the in-plane compressive residual stress produced by the misfit strain between the bulk and the subsurface material [2]. The GNS subsurface layer can be formed through surface strengthening treatments by means of mechanical methods such as shot peening (SP), which entails impacting a surface with small, round, and hard particles with force sufficiently high to create localized plastic deformation for the formation of a deep work-hardened and compressed subsurface layer in metals and alloys [3, 4]. In the recent several years, there have been many new types of peening techniques such as laser shock peening, ultrasonic shot peening, water cavitation peening, and severe shot peening which uses more intense parameters compared to conventional shot peening [5–8]. Despite the development of these new variants, conventional shot peening method remains one of the most important means in the industrial production due to its high flexibility and productivity, low cost, and environmental friendliness. For these reasons, shot peening process is of particular interest in the present work.

Mechanical methods can be combined with other surface strengthening treatments such as thermochemical methods for further improvement in fatigue strength and fatigue life of steel components [9–13]. As the thermochemical method is mostly benefited by increasing the microhardness and the mechanical method is mostly benefited by generating the compressive residual stress, a positive synergistic effect can therefore be anticipated if these two methods are combined. It is highlighted that compared with the single mechanical method, the combination of mechanical and thermochemical methods can be more advantageous in terms of not only the microhardness and residual stress distributions, but

Table 1: Chemical composition of 18CrNiMo7-6 steel.

Element	C	S	Si	Mn	P	Cr	Ni	Mo	Fe
Composition (Wt.%)	0.15–0.21	≤0.035	≤0.40	0.50–0.90	≤0.025	1.50–1.80	1.40–1.70	0.25–0.35	Balance

Table 2: Shot peening parameters for case-hardened 18CrNiMo7-6 steel.

Variant	Shot diameter (mm)	Coverage (%)	Almen intensity (mmA)
SP0	—	—	—
SP1	0.3	200	0.25
SP2	0.6	200	0.25
SP3	0.6	200	0.45

also the overall mechanical properties, and the hybrid process can finally obtain a remarkable improvement of fatigue limit for surface treated low-alloy steel regardless of the sequence how nitriding and severe shot peening are combined [10]. However, the hybrid process cannot be always advantageous to the application of steels. For instance, it is shown in [11] that when both carbonitrided gear and carbonitrided plus peened gear made of AISI 4130 steel are subjected to contact fatigue testing, fatigue damages, which are ought to be in different modes, are found to occur after about the same testing time for both types of methods. This could most probably be a consequence of the use of inappropriate shot peening condition; the extreme shot bombardment on the surface can cause roughness increment and flaw occurrence and therefore outweigh the beneficial effect brought by the hybrid process. Therefore, efforts are made in the present work to address the issue questioning the appropriate mechanical process condition that should be selected posterior to thermochemical method in order to maximize its beneficial effect on the fatigue life improvement of structural metallic materials.

Thus, the selection of an optimal mechanical process condition which enhances the fatigue performance of case-hardened steels is the main concern of the present work, with the ultimate aim to understand from an experimental point of view how the mechanical process parameters affect the heat-treated surface and subsurface layer properties, which in turn influence the fatigue performance. To tackle this issue, high-strength 18CrNiMo7-6 steel, widely employed in high-speed and heavy-duty gear applications, is selected as the target material. The carburizing and shot peening are respectively selected as thermochemical and mechanical methods since they are the versatile surface strengthening treatments commonly used in the automotive industry. In the present work, a few single shot peening conditions with different Almen intensities and shot diameters, which are recognized as ones of the measurable key parameters of shot peening process, are carried out on 18CrNiMo7-6 steel posterior to the carburizing process. By carrying out the surface and subsurface layer property analysis and fatigue testing, this work is aimed at establishing qualitative interrelationships between peening process conditions, surface and subsurface layer properties, and fatigue performance. Subsequently, based on the obtained qualitative relationships, we propose an optimized dual peening condition that can produce superior surface and subsurface layer properties characterized by work hardening, compressive residual stress, microstructural alteration, and surface roughness, leading to not only longer service lifetime but also smaller dispersion degree of fatigue life data. The proposed protocol is demonstrated and validated on industrial gears, which can be valuable for providing a design guideline for engineering industries.

2. Experiment Setup

2.1. Material. In the present study, the target material is 18CrNiMo7-6 steel and the supplier-given raw material chemical composition is summarized in Table 1. All the specimens are carburized in a controllable gas carburizing furnace, then subsequently quenched in oil to room temperature, and finally followed by tempering and cooling in air. The thermochemical conditions are utilized in agreement to gear heat treatment standard ANSI/AGMA B89-2004 [14].

2.2. Shot Peening Treatment. The shot peening treatment is performed with the air blast shot peening machine. The specimens are treated by shot peening with different intensities and shot diameters. The intensities of peening are measured by the arc height of Almen specimens, varying from 0.25 mmA to 0.45 mmA. Cast steel balls with diameters of 0.3 mm and 0.6 mm are selected as shot blasting media in accordance to ISO 26910-1 [15]. The coverage of shot peening is 200% for all peening processes, which is obtained by doubling the exposure time needed to achieve full coverage (100%). Note that the roughness increases gradually with the increasing degree of coverage until reaching full coverage and remains constant thereafter, and thus, to ensure that the specimens can benefit fully the advantages of the applied surface treatment methods in terms of subsurface layer properties, it is of prime importance to keep constant the level of the generated surface roughness [16]. The different shot peening configurations of immediate interest, which are determined based on the previous laboratory testing, are presented in Table 2.

2.3. Measurement Methods. The specimens under test are gear teeth prepared using wire-cut electrical discharge machining, the cut surface area of the specimen being located far away from the surface area of interest. The cross-section of the specimen is first mechanically polished using standard metallographic techniques, then chemically etched by 8% Nital.

The cross-section microstructure of the specimen is subsequently investigated by optical microscopy (OM) and scanning electron microscopy (SEM) using Zeiss Auriga FIB-SEM at room temperature.

The microhardness is measured along the depth of the cross-section of the specimen using a Vickers microhardness tester with a load of 200 g and a holding time of 10 s. Considering the material's heterogeneities and measurement errors, three microhardness measurements are acquired at each depth, whose average values are used in this work.

The residual stress is measured by the X-ray stress analyzer (LXRD, Proto, Canada) using Cr Kα radiation and martensitic {211} crystalline plane. The voltage and current are, respectively, 30 kV and 25 mA. The measured interference peaks are evaluated by the sin 2ψ method with the diffraction angle (2θ) varying from -45° and 45°. The in-depth profiles of the residual stresses are determined by performing first iterative electrolytic removal of thin surface layers followed by X-ray in-depth measurements.

In addition to the analysis of the cross-section area performed on the specimen, the surface state of the specimen is examined by Veeco Wyko NPFLEX optical profiler. The measured surface topography is characterized by amplitude surface roughness parameters in agreement with ISO 25178-2012 [17], which are frequently used to measure the vertical characteristics of the surface deviation [18]. Taking into account the spatial surface roughness variations, the presented surface roughness data are the values averaged over three measurement zones on each specimen.

2.4. Fatigue Testing. Following the setup and procedure for conducting the SAE single-tooth bending fatigue test (cf. Figure 1) using a servohydraulic fatigue testing machine [19], the applied cyclic fatigue load is 0.82 of the yield stress of the bulk material, the stress ratio $R = 0.01$, and the nominal cyclic frequency is 89 Hz at room temperature. Each test series includes six gear tooth specimens. All the specimens are tested until occurrence of fracture, else the tests are terminated at 3×10^6 cycles.

3. Results and Discussions

3.1. Microstructure. In Figure 2, the cross-sectional surface by SEM is presented for carburized specimen, where three distinct regions with different microstructures can be recognized. As can be seen in Figure 2(a), a very thin white carbon oxide layer of a few microns is formed at the top surface; the pores, carbide particles, and microcracks are presented within the oxidized layer, as exhibited in the inserted figure of Figure 2(a). Beneath the oxidized layer is known as the so-called case-hardened zone, which consists mainly of martensite microstructure with a very small quantity of retained austenite and finely dispersed undissolved spherical carbide particles. In the innermost zone, the substrate without any evidence of microstructural change is observed (cf. Figure 2(b)).

Though carburizing technique has generally a beneficial effect on the fatigue behavior of specimens, the oxidized layer and the remained amount of retained austenite can be detrimental to high-cycle fatigue, as the presence of the retained austenite can decrease the elastic limit and the yield strength [20]. For this reason, shot peening, a cold working process consisting of bombarding a ductile surface with numerous hard particles at velocity sufficiently high to create localized plastic deformation, is often performed posterior to carburizing. Considering the high brittleness of oxidized layer, the impingement of hard shot particles on the outermost surface layer could sometimes cause the formation of highly damaged surface area covered with plenty of microcracks if inappropriate shot peening condition is selected.

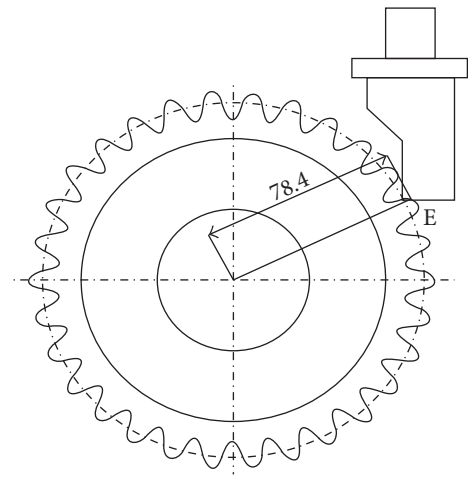

Figure 1: Schematic diagram of the bending fatigue testing of the cylindrical gear.

Figure 3 presents SEM micrographs of the cross-section of carburized 18CrNiMo7-6 steel after shot peening treatment. From Figure 3(a), it can be found that shot peening performed after carburizing can not only suppress the porous structure and eliminate the carbide particles at the outer oxidized layer, but also modify the microstructure of the near surface region of case-hardened 18CrNiMo7-6 steel; the plastic deformation-induced grain refinement and strain-induced phase transformation are the principal microstructural changes that occur during shot peening treatment, which are well recognized to be a consequence of the accumulated localized plastic strain caused by the repeated impingement by shot particles on the specimen surface. This shows that shot peening allows not only improving the material response, but also modifying the microhardness and (residual) stress fields as discussed later; the results are similar to [4, 21].

Shot peening is a process which projects high-velocity shot particles by the action of an external force. So, when the external force reaches the critical stress required for dislocation movement, dislocation slip is generated, and well-defined slip band structure is therefore formed. On the same slip plane, when the amount of dislocations impeded at the grain boundaries increases, the pile-ups of dislocations are formed [22]. Consequently, the phenomenon of stress concentration can easily occur in the vicinity of grain boundaries due to the heavy accumulation of the dislocations pile-ups against the boundaries. When a critical stress value is reached, the grain boundaries are destroyed and a high-density nanoscale deformation twins is formed. The intensive interactions between twin boundaries and dislocations can then lead to subsequent transformation of

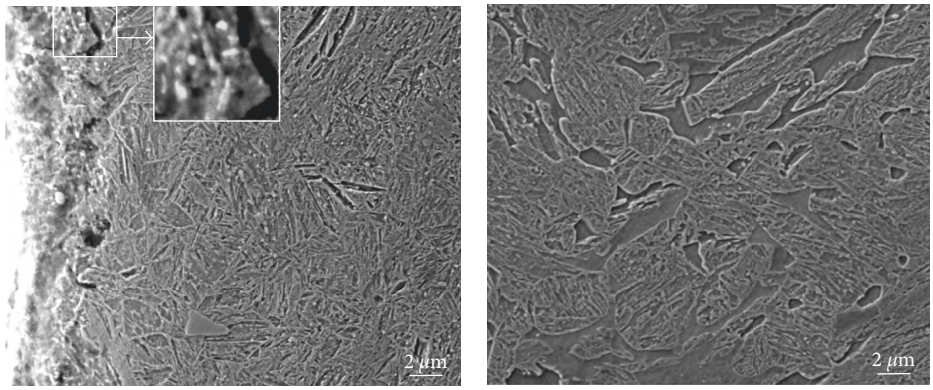

(a) (b)

Figure 2: Cross-sectional SEM of carburized SP0 specimen; the microstructure of (a) top surface region and (b) bulk material, with the inserted image in (a) showing an enlarged representation of pores, carbide particles, and microcracks.

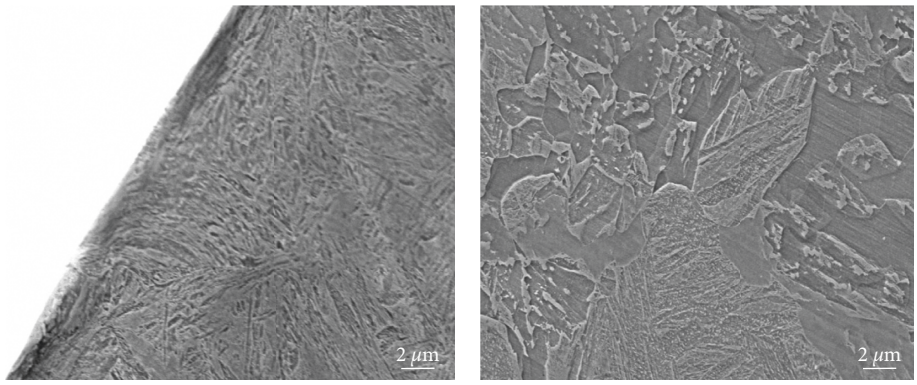

(a) (b)

Figure 3: Cross-sectional SEM of carburized and peened SP3 specimen; the microstructure of (a) top surface region and (b) bulk material.

two-dimensional twin lamellae structures into three-dimensional nanograins with their boundary characteristics lying in the form of low angle and high angle. Herein, there is a considerable fraction of low-angle grain boundaries and a high density of dislocations resided in the nonequilibrium high-angle grain boundaries [23]. In addition to plastic deformation-induced grain refinement, strain-induced phase transformation is another mechanism by which nanosurface forms during shot peening. The strain-induced nucleation of martensite transformation can take place more dominantly at higher-energy grain boundaries due to their atomic structures and energies. Besides, the strain localization bands and deformation twins that accumulate high strain energy storage could also promote martensitic transformation. All these are elaborated here to show that the principal microstructural changes induced by shot peening consist of plastic deformation-induced grain refinement and strain-induced phase transformation.

In general, the microstructure is deemed to have a strong correlation with the microhardness, where the former's modification can be reflected by the change of the latter [22]. Due to the reduction of the content of retained austenite caused by martensite transformation and austenite grain refinement led by the shot peening process, a microhardness improvement at the top surface region of carburized and peened specimens is clearly present, as is detailed in the next section.

3.2. Hardness. Conventionally, the microhardness value is used to characterize the work-hardened properties. In some cases, the size of the microhardness marks impressed along the depth direction of the subsurface layer can also be considered as an option used to illustrate very roughly the variation of the microhardness along the depth direction. Thereby, it is presented in Figure 4 the distributions of the in-depth microhardness of all specimens. For carburized-only SP0 specimens, the maximum microhardness appears on the surface (denoted as maximum surface microhardness), then gradually decreases with increasing depth and finally reaches a stabilized value. It is well accepted that this is mainly due to the declination of the carbon content from the surface to the center. Meanwhile, when shot peening is performed on case-hardened steels, regardless of shot peening condition, a similar trend of the microhardness distribution is observed. This can generally be attributed to the peening-induced reduction of plastic deformation from the outer surface to the center due to the lower grain refinement, martensite transformation, and dislocation density when approaching the center.

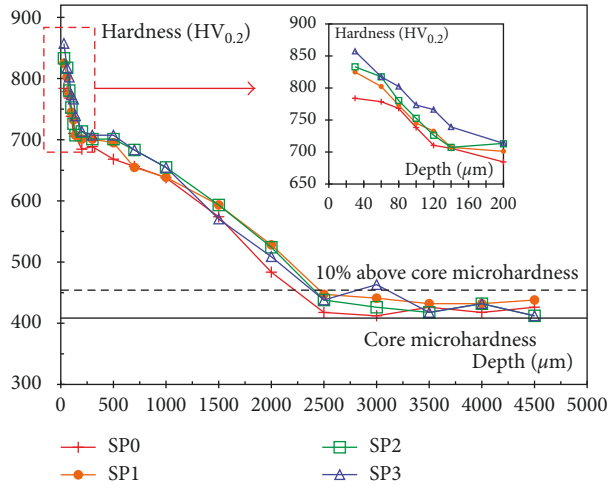

Figure 4: Microhardness distribution curves of all surface treated specimens.

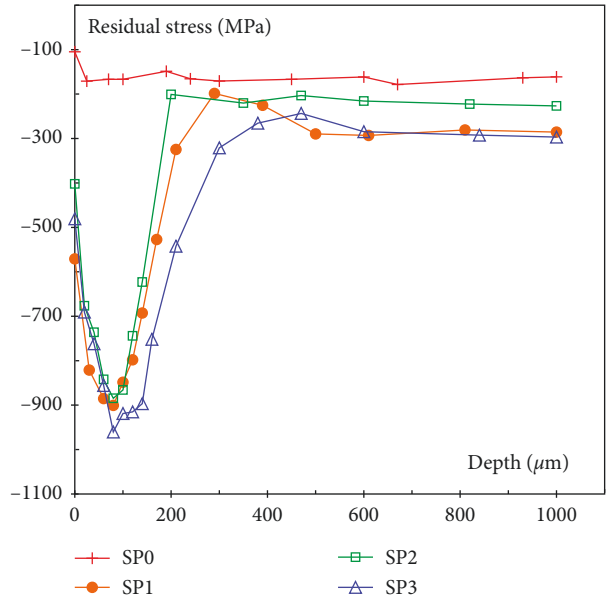

Figure 5: Residual stress distributions of all surface treated specimens.

Case depth after thermochemical treatments is very often considered as a matter of convention. When fatigue performance is oriented, a microhardness value of 10% above the core microhardness is generally used to characterize the case depth [13]. The case depth is approximated to be ~2250 μm, as exhibited in Figure 4. It is shown that the case depth is remained unchanged after shot peening is carried out posterior to carburizing.

In comparison to the single carburizing process, the hybrid process of carburizing and shot peening has caused an improvement in surface microhardness, in particular maximum surface microhardness, from the top surface up to a limited depth estimated to ~140 μm, as clearly seen in the inserted image of Figure 4. Compared to the maximum surface microhardness of carburized-only SP0 specimens (784 $HV_{0.2}$), that of carburized and peened are estimated to increase by 9.3% for SP3 specimens (857 $HV_{0.2}$), by 6.3% for SP2 specimens (833 $HV_{0.2}$), and by 5.2% for SP1 specimens (825 $HV_{0.2}$). The improvement in surface microhardness can be attributed to the peening-induced microstructural changes in the hardened surface region due to the reduction of the content of retained austenite caused by martensite transformation and austenite grain refinement. Refer to Figure 3(a) for a very dense structure consisting mainly of the martensitic state formed on the hardened top surface region after shot peening.

Regarding the two peening parameters (shot diameter and Almen intensity), it can be seen that the increase in the maximum surface microhardness caused by the increase of shot diameter is quite comparable to that resulted by the increase of Almen intensity. Indeed, the values of the maximum surface microhardness are found to increase by ~2.9% with the increment of the Almen intensity and by ~1.0% with the increase of the shot diameter, which shows that the maximum surface microhardness increment is restricted to some extent. This finding infers that the plastic deformation of 18CrNiMo7-6 steel subjected to the combined processing of carburizing and shot peening has reached a critical condition. Indeed, when the hardened region near the surface is treated with shot peening, a very small plastic deformation is produced. This is because the hardened surface region can no further accumulate localized plastic strain during the peening process due to the presence of a very high dislocation density and carbon content induced by the prior carburizing process, resulting in a slight increase in the maximum surface microhardness. The results hereby obtained show that the thermochemical surface treatment is advantageous in terms of microhardness distribution compared to mechanical surface treatment, which is consistent with the results obtained in [10].

3.3. Residual Stress. In Figure 5, the in-depth distributions of the residual stress for all the surface treated specimens are depicted. In the range of testing, all the specimens are found to have similar trend of obvious compressive residual stress distribution; the top surface compressive residual stress first increases to a maximum (denoted as maximum compressive residual stress), then decreases gradually along the depth direction of the hardened layer and remains constant thereafter.

From Figure 5, both the top surface compressive residual stress and maximum compressive residual stress are exhibited to be much more important for the hybrid processing of carburizing and shot peening than the individual carburizing process. This observation shows that shot peening process is highly beneficial in forming compressive residual stress as compared with the carburizing process which is previously seen to be responsible for increasing microhardness. The compressive residual stress is well recognized to be related to the plastic deformation, due to the creation of an elevated level of the plasticity unevenness; it can subsequently give rise to compressive residual stress in the steel [24]. In general, two types of plastic deformations can be distinguished [25]: (i) plastic deformation due to surface hammering which tends to localize the peak on the surface and (ii) plastic deformation induced by Hertzian pressure which is responsible for the

subsurface peak. Yet, in the case of shot peening performed posterior to carburizing, a third process heavily linked with the content of retained austenite is considered as predominant especially in generating compressive residual stress; that is, the intensity of the local stress field produced by the impacts of shot peening can trigger the diffusionless phase transformation from austenite to martensite [26]. As a result of the constraint exerted by the surrounding material on the volume expansion, the compressive residual stress would then become deeper [21]. Consequently, the peak of the residual stress would then be seen moving to the region where the Hertzian pressure is the highest.

Regardless of the shot peening process parameter, the values of the compressive residual stress are shown to be lower at the top surface than at the peak position, and the maximum compressive residual stresses are found to be located in the subsurface region at the depth of ~90 μm. The former is most likely a consequence of the counteracting effects by tensile residual stress and high surface roughness produced by prior machining processes. And the latter suggests that the steel material, which undergoes plastic deformation, has most probably reached a critical plastic deformation limit, and thus the continuous impingement of the shot particles does not further deepen the compressed subsurface region.

In Figure 5, the values of the compressive residual stress observed at the top surface and peak position increase with Almen intensity. This is because the increase in Almen intensity, which accelerates the shot velocity, produces more kinetic energy and thereby induces a greater amount of plastic deformation on the hardened surface region. However, with an increase of the shot diameter, the top surface and maximum compressive residual stresses are on the decrease. One of the reasons for this phenomenon is that when larger diameter shots are projected on the surface of specimens with a small-scale finite kinetic energy, a larger impact area is created. Thereby, it can result in a reduction of equivalent plastic strain and consequently the compressive residual stress is lowered. Besides, from Figure 5, it can be seen at the top surface region that the effect of shot diameter is more significant than that of Almen intensity on the compressive residual stress; the decrease of shot diameter induces an increase of compressive residual stress by 42.0% while the increase of Almen intensity causes an increase of compressive residual stress by only 19.7%. It can also be observed from Figure 5 that the values of the compressive residual stress at the peak position (~90 μm) appear to be less severely affected by shot diameter rather than Almen intensity; the increase of Almen intensity leads to an increase in compressive residual stress by 8.5% while the compressive residual stress grows by only 1.8% with the decrease of shot diameter.

3.4. Roughness. In what follows, the roughness characterization results are presented for both the individual carburizing and the hybrid process of carburizing and shot peening. The surface roughness parameter S_a, which denotes the arithmetic mean height and is the counterpart of the parameter arithmetical mean deviation of the roughness profile (R_a), is a commonly used roughness parameter for characterization of measured surface textures. Thus, S_a is used in what follows to discuss the surface states of treated specimens. In Table 3, the values of S_a are presented. For the specimen SP0 with the S_a value of ~2.51 μm, the surface of carburized specimens can be considered as rather rough. In this instance, the roughness can be ascribed to the texture left by machining (cf. Figure 6(a)) but also to the formation of the oxide layer produced during carburizing process (cf. Figure 2(a)).

Table 3: Values of the surface roughness parameter S_a of all surface treated specimens.

Variant	SP0	SP1	SP2	SP3
S_a (μm)	2.51	1.97	2.69	1.89

It can be seen from Table 3 that the magnitude of roughness due to shot peening induced at the carburized specimen surface depends on applied shot peening conditions. The surface roughness of SP1 specimens (with $S_a \approx 1.97\,\mu$m, cf. Figure 6(b)) is exhibited to decrease by 21.5% compared to that of SP0 specimens (with $S_a \approx 2.51\,\mu$m, cf. Figure 6(a)). This can be attributed to the fact that when Almen intensity is low, the impact of shot peening using smaller shot blasting particles is equivalent to the effect of surface polishing, which is however unable to induce sufficient plastic deformation that allows modifying completely the surface texture left by heat treatments and machining operations (cf. Figure 6(b)). In contrast, if shot peening process is performed using larger shot blasting particles, the surface roughness is increased. So the roughness of SP2 specimens (with $S_a \approx 2.69\,\mu$m, cf. Figure 6(c)) is found to be 36.5% higher than that of SP1 specimens. This is because the use of larger shot media can produce a higher level of surface plastic deformation that allows not only to enhancing the magnitude of the surface roughness increment, but also to obtaining a more evenly distributed texture, as illustrated in Figure 6(c).

With increasing Almen intensity from 0.25 mmA to 0.45 mmA, the surface state of the specimens is improved, and the surface roughness is thus reduced. For example, the S_a value of SP3 specimens ($\approx$1.89 μm, cf. Figure 6(d)) is approximated to be 29.7% less than that of SP2 specimens. This can be explained by the fact that the hard heat-treated surface region has been subjected to the so-called "intense" shot peening process condition. It is worth noting that using a high Almen intensity at double coverage can be interpreted as if every portion of the hard surface region has been treated with very high impact energy shot blasting particles for at least two times. Thereby, when the hard surface region is intensely shot peened, only a small amount of plastic deformation is induced as a consequence of the attainment of a critical limit of the plastic deformation, and as a result, the surface roughness is difficultly being altered. Due to the continuous impingement of the shot particles on the specimen surface, the surface state is thereby improved with lowered surface roughness (cf. Figure 6(d)). This observation is found to be in accordance with the results exhibited in the literature [9, 10, 27].

3.5. Fatigue Test Data. The fatigue tests are carried out to examine the fatigue performance of all the surface treated

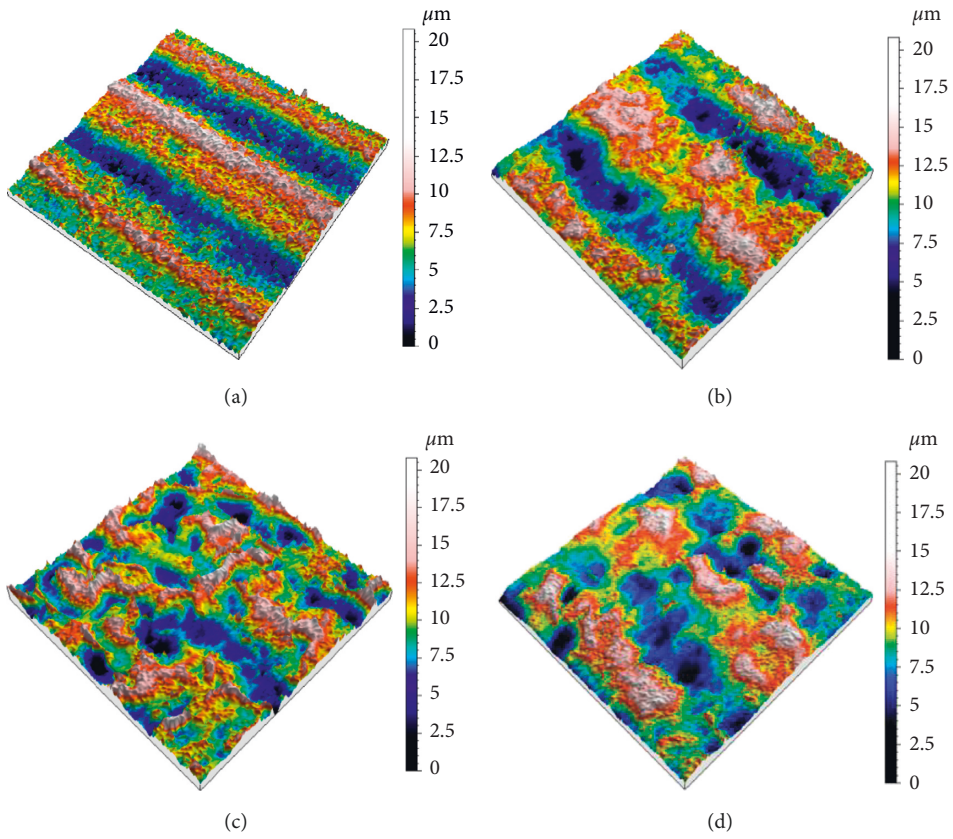

Figure 6: Surface topographies at the root surfaces of (a) SP0, (b) SP1, (c) SP2, and (d) SP3 specimens.

specimens. In Figure 7, the fatigue lives (N_f) of these surface treated specimens are depicted. N_f for case-hardened specimens is determined in the range of $14.8–57.9 \times 10^3$ cycles. It is noticeable that the shot peening process can considerably improve the fatigue lives of case-hardened specimens, which is attributed to the microstructure refinement, retained austenite reduction, microhardness amelioration, compressive residual stress generation, and surface roughness alteration induced by shot peening processes. These improved attributes are revealed to exhibit beneficial effects on fatigue strength and bending fatigue life [28]. It is worth noting that the trend of fatigue life improvement is highly dependent on the surface and subsurface layer properties which are controlled by shot peening conditions.

It is clearly shown in Figure 7 that N_f for SP2 specimens is the lowest, and it is improved by increasing Almen intensity, as exhibited by SP3 specimens. This significant improvement is solely a consequence of the presence of deeper compressed work-hardened subsurface layer with ameliorated surface roughness in SP3 specimens. Meanwhile, SP1 specimens are found to have the highest N_f despite the moderate work hardening and compressive residual stress. The remarkable increase in N_f for SP1 specimens can be related to the fact that the magnitude of the surface roughness is the lowest among all peened specimens (cf. Table 3). Nevertheless, the dispersion of the fatigue life of SP1 specimens is found to be rather large; the longest lifetime is estimated to be

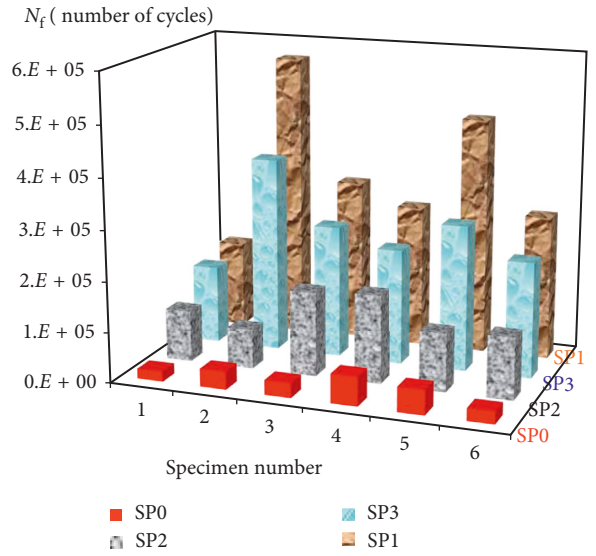

Figure 7: Bending fatigue lives of surface treated specimens.

about 69% more than the shortest one. However, the variation scale of the fatigue data obtained for SP1 specimens can be considered to be rather similar to the level of the fatigue data reported on shot peening [29, 30].

The presence of the scatter in the fatigue life can originate from the peening induced average surface and subsurface layer properties. Two important uncertain sources are noted here.

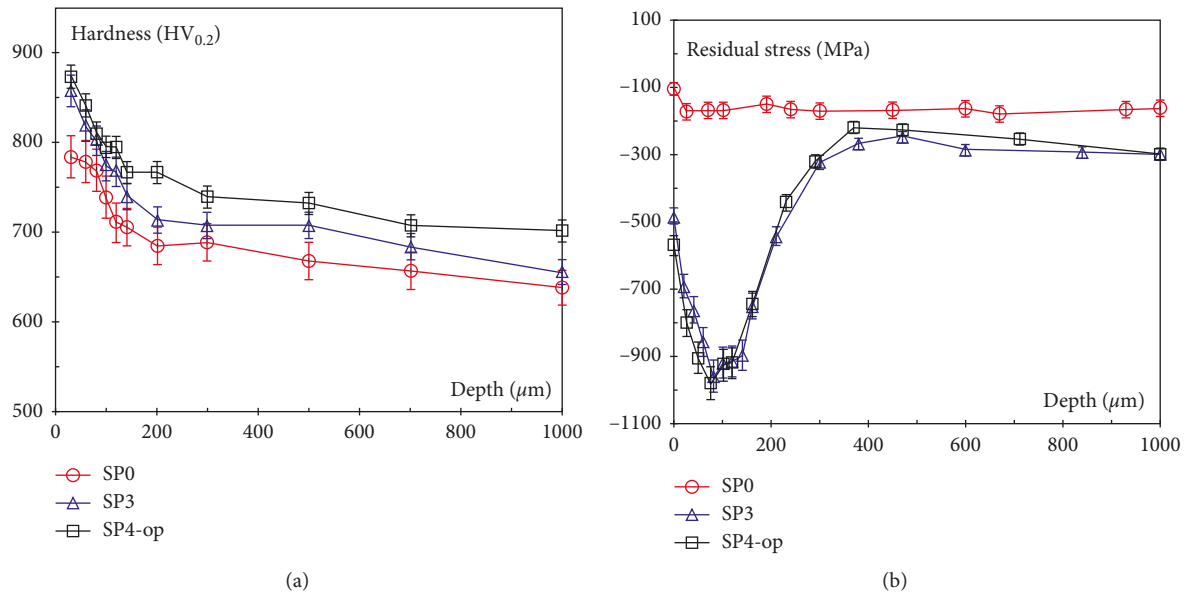

Figure 8: In-depth (a) microhardness and (b) residual stress distributions of the surface treated specimens.

One is the nonuniformity of the subsurface layer property, in particular, the uneven spatial distribution of the compressive residual stress. It is recently shown by [31] that if shot peening causes the unevenness of the residual stress distribution in a very small region of the surface, this can neutralize the beneficial effect of the compressive residual stress and hence degrade the fatigue resistance. The other is the fatigue strength endowed by the surface and subsurface layer properties, which is unable to completely cause a shift in fatigue crack initiation site from a surface to subsurface location and therefore cause the simultaneous occurrence of both surface and subsurface fatigue crack initiation in a fatigue testing series. This certainly intensifies the dispersion of the fatigue life.

3.6. Determination of Optimal Shot Peening Process

3.6.1. Optimal Shot Peening Conditions. In the previous section, it is investigated that the peening induced surface and subsurface layer properties can shift the fatigue life; it is of particular importance to optimize the shot peening conditions with the purpose to maximize their beneficial effect for enhanced fatigue performance. The testing results indicate that on one hand, SP1 specimens, possessing a moderate subsurface layer properties with reduced surface roughness, exhibit a considerable improvement in fatigue life which is however associated with a rather large scatter, and on the other hand, SP3 specimens, owing to its superior subsurface layer properties with rather low surface roughness, have a comparable estimate of the fatigue life with a moderate scatter. These investigations motivate us to propose an optimal shot peening conditions by grouping different peening conditions. The proposed dual peening process consists of two steps, as indicated by the name. The first peening process is aimed at generating a deep compressed work-hardened subsurface region by using a large media with very high kinetic energy, that is, with SP3

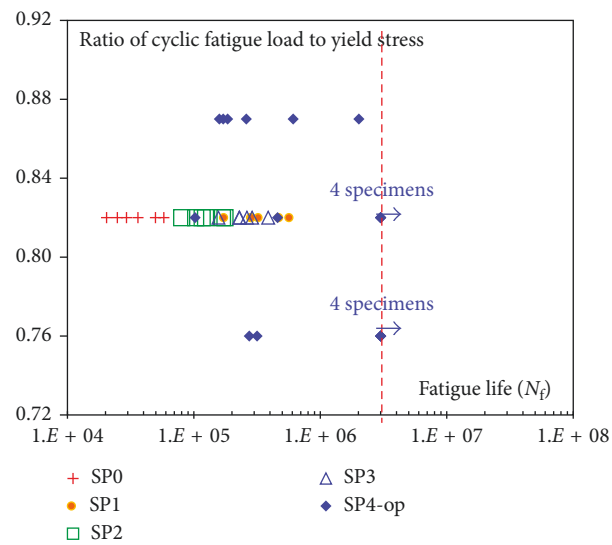

Figure 9: The ratio of applied cyclic load to yield stress versus fatigue life data.

process, and the repeening process is then performed using a smaller media with rather low kinetic energy, that is, with SP1 process, in order to improve the surface state (e.g., reduce the roughness and enhance its uniformity).

3.6.2. Validity of the Proposed Solution. In the following, the specimens subjected to the proposed optimal shot peening condition are denoted as SP4-op specimens. The experimental results show that the maximum microhardness of 874 $HV_{0.2}$ appears on the surface (cf. Figure 8), the values of top surface and maximum compressive residual stresses are, respectively, 569 MPa and 980 MPa, and the estimated value of S_a is equal to ~1.86 μm. Compared to the previous single peening method, the dual peening method by using first

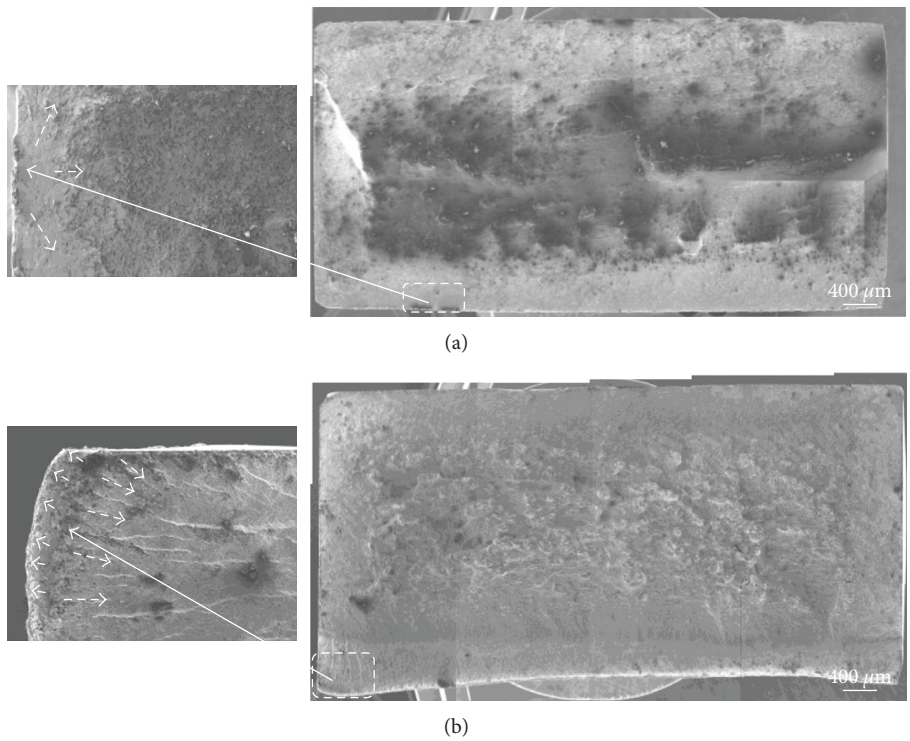

Figure 10: SEM micrographs of the surface treated specimens obtained at the ratio of applied cyclic load to yield stress of (a) 0.87 and (b) 0.82.

a large media with very high kinetic energy followed by a smaller media with rather low kinetic energy can indeed be more advantageous in producing improved quality of the surface and subsurface layer of 18CrNiMo7-6 steel. It is emphasized that the repeening process in the dual peening method has double benefits: firstly, inducing a more regular surface state by smoothing sharp corners and somehow closing the microcracks generated during the first shot peening process; secondly, generating a more homogeneous surface residual stress and surface microhardness [29, 32].

To validate the proposed shot peening process condition for fatigue life enhancement, the fatigue test is carried out for SP4-op specimens under three different stress levels; the ratio of the applied cyclic fatigue load to yield stress is 0.76, 0.82, and 0.87. The fatigue data presented in Figure 9 show that for the first two cyclic load levels, the bending fatigue life of gear teeth is greatly improved, that is, not only the fatigue life is increased marvelously (with $N_f \geq 3 \times 10^6$ cycles), but also the degree of dispersion in the fatigue-life data is also minimized. This affirms the capability of the dual peening process in delaying the fatigue crack initiation phase by enhancing the surface and subsurface layer properties of 18CrNiMo7-6 steel. However, when the ratio of applied cyclic fatigue load to yield stress is increased up to 0.87, the fatigue performance of SP4-op specimens is drastically degraded.

The aforementioned observations are understood as follows. Under the high cyclic fatigue load, fatigue cracks are most likely to initiate from the surface (cf. Figure 10(a)), in contrast to the case of lower fatigue loads, where fatigue cracks are found to be prone to originate from the interior of the subsurface layer region (cf. Figure 10(b)). When the load level is low, the peak stress of the applied fatigue load does not exceed the increased fatigue strength at the surface; however, at some depth below the surface, the applied stress can be larger than the local fatigue strength. Using the concept of the local fatigue strength applied for surface treated material [10], the intersection of the applied stress level with the local fatigue strength curve gives the site of crack initiation; subsurface crack initiation does occur. In the case of high load being applied, crack initiation happens at the surface because the peak stress at the free surface exceeds the increased fatigue strength.

4. Conclusion

In this paper, the effect of different shot peening conditions on the surface and subsurface layer properties and the fatigue performance of case-hardened 18CrNiMO7-6 steel has been investigated. The analysis of the surface and subsurface integrity reveals that the subsurface region of the case-hardened 18CrNiMO7-6 steel can no further accumulate enormous localized plastic deformation during shot peening process as a consequence of the attainment of a critical limit of the plastic deformation for 18CrNiMo7-6 steel due to the presence of a high dislocation density and carbon content induced by the prior carburizing process. Based on the quantitative assessment of subsurface layer properties and fatigue performance, the interrelationships between peening process, subsurface layer properties, and fatigue performance are qualitatively established; shot peening application with lower intensity and smaller shots causing moderate subsurface layer properties results in an increase in both

fatigue life and its associated scatter, while shot peening application with higher intensity and larger shots producing superior subsurface layer properties exhibits comparable estimate of fatigue life with decreased scatter in fatigue data. The experimental study suggests that a two-step shot peening process, where a large media with very high kinetic energy is used in the first step and a smaller media with rather low kinetic energy in the second step, can be considered as an effective way to enhance the surface and subsurface layer characteristics and the fatigue performance; the optimality of the proposed dual peening process is experimentally validated and discussed.

Conflicts of Interest

The authors declare that they have no conflicts of interest.

Acknowledgments

The authors are grateful to the National Natural Science Foundation of China–International Cooperation and Exchange Program (Grant no. 51650110502) and Henan Provincial Research Bureau (Grant nos. 15A460030 and 17A460025) for their financial support.

References

[1] K. Lu, "Making stronger materials ductile with gradients," *Science*, vol. 345, no. 6203, pp. 1455-1456, 2014.

[2] T. Hanlon, E. D. Tabachnikova, and S. Suresh, "Fatigue behavior of nanocrystalline metals and alloys," *International Journal of Fatigue*, vol. 27, no. 10–12, pp. 1147–1158, 2005.

[3] Y. K. Gao and X. R. Wu, "Experimental investigation and fatigue life prediction for 7475-T7351 aluminum alloy with and without shot peening-induced residual stresses," *Acta Materialia*, vol. 59, no. 9, pp. 3737–3747, 2011.

[4] P. Fu, K. Zhan, and C. H. Jiang, "Micro-structure and surface layer properties of 18CrNiMo7-6 steel after multistep shot peening," *Materials and Design*, vol. 51, pp. 309–314, 2013.

[5] S. Huang, Y. Zhu, W. Gui et al., "Effects of laser shock processing on fatigue crack growth in Ti-17 titanium alloy," *Journal of Materials Engineering and Performance*, vol. 25, no. 2, pp. 813–821, 2017.

[6] V. Singh and M. Marya, "Surface modification of oilfield alloys by ultrasonic impact peening: UNS N07718, N07716, G41400 and S17400," *Journal of Materials Engineering and Performance*, vol. 25, no. 1, pp. 338–347, 2016.

[7] S. J. Kim, K. Y. Hyun, and S. K. Jang, "Effects of water cavitation peening on electrochemical characteristic by using micro-droplet cell of Al-Mg alloy," *Current Applied Physics*, vol. 12, pp. S24–S30, 2012.

[8] L. Trsko, M. Guagliano, O. Bokuvka, F. Novy, M. Jambor, and Z. Florkova, "Influence of severe shot peening on the surface state and ultra-high-cycle fatigue behavior of an AW 7075 aluminum alloy," *Journal of Materials Engineering and Performance*, vol. 26, no. 6, pp. 2784–2797, 2017.

[9] Y. Lv, L. Q. Lei, and L. N. Sun, "Influence of different combined severe shot peening and laser surface melting treatments on the fatigue performance of 20CrMnTi steel gear," *Materials Science and Engineering A*, vol. 658, pp. 77–85, 2016.

[10] S. M. Hassani-Gangaraj, A. Moridi, M. Guagliano, A. Ghidini, and M. Boniardi, "The effect of nitriding, severe shot peening and their combination on the fatigue behavior and microstructure of a low-alloy steel," *International Journal of Fatigue*, vol. 62, pp. 67–76, 2014.

[11] A. C. Batista, A. M. Dias, J. L. Lebrun, J. C. Le Flour, and G. Inglebert, "Contact fatigue of automotive gears: evolution and effects of residual stresses introduced by surface treatments," *Fatigue and Fracture of Engineering Materials and Structures*, vol. 23, no. 3, pp. 217–228, 2000.

[12] P. G. Ranaware and M. J. Rathod, "Combined effect of shot peening, subcritical austenitic nitriding, and cryo-treatment on surface modification of AISI 4140 steel," *Materials and Manufacturing Processes*, vol. 32, no. 4, pp. 349–354, 2017.

[13] F. Ashrafizadeh, "Influence of plasma and gas nitriding on fatigue resistance of plain carbon (Ck45) steel," *Surface and Coatings Technology*, vol. 174-175, pp. 1196–1200, 2003.

[14] ANSI/AGMA B89, *Gear Material and Heat Treatment Manual*, American Gear Manufacturers Association, Alexandria, VI, USA, 2004.

[15] ISO 26910-1, *Springs–Shot Peening–Part 1: General Procedures*, International Organization for Standardization, Geneva, Switzerland, 2009.

[16] V. Llaneza and F. J. Belzunce, "Study of the effects produced by shot peening on the surface of quenched and tempered steel: roughness, residual stress and work hardening," *Applied Surface Science*, vol. 356, pp. 475–485, 2015.

[17] ISO 25178-2, *Geometrical Product Specifications (GPS)–Surface Texture: Areal–Part 2: Terms, Definitions and Surface Texture Parameters*, International Organization for Standardization, Geneva, Switzerland, 2012.

[18] E. S. Gadelmawla, M. M. Koura, T. M. A. Maksoud, I. M. Elewa, and H. H. Soliman, "Roughness parameters," *Journal of Materials Processing Technology*, vol. 123, no. 1, pp. 133–145, 2002.

[19] R. W. Buenneke, M. B. Slane, C. R. Dunham, M. P. Semenek, M. M. Shea, and J. E. Tripp, "Gear single tooth bending fatigue test," in *Proceedings of SAE Technical Paper 821042*, Milwaukee, WI, USA, 1982.

[20] M. Zaccone and G. Krauss, "Elastic limit and microplastic response of hardened steels," *Metallurgical and Materials Transaction A*, vol. 24, no. 10, pp. 2263–2277, 1993.

[21] M. Benedetti, V. Fontanari, B. R. Hohn, and T. Tobie, "Influence of shot peening on bending tooth fatigue limit of case hardened gears," *International Journal of Fatigue*, vol. 24, no. 11, pp. 1127–1136, 2002.

[22] S. M. Hassani-Gangaraj, K. S. Cho, H. J. L. Voight, M. Gugliano, and C. A. Schuh, "Experimental assessment and simulation of surface nanocrystallization by severe shot peening," *Acta Materialia*, vol. 97, pp. 105–115, 2015.

[23] X. H. An, Q. Y. Lin, S. D. Wu, and Z. F. Zhang, "Improved fatigue strengths of nanocrystalline Cu and Cu-Al alloys," *Materials Research Letters*, vol. 3, no. 3, pp. 135–141, 2015.

[24] K. Dalaei, B. Karlsson, and L. E. Svensson, "Stability of shot peening induced residual stresses and their influence on fatigue lifetime," *Materials Science and Engineering A*, vol. 528, no. 3, pp. 1008–1015, 2011.

[25] M. Kobayashi, T. Matsui, and Y. Murakami, "Mechanism of creation of compressive residual stress by shot peening," *International Journal of Fatigue*, vol. 20, no. 5, pp. 351–357, 1998.

[26] R. E. Reed-Hill and R. Abbaschian, *Physical Metallurgy Principles*, Publishing Company, Boston, MA, USA, 1992.

[27] O. Unal and R. Varol, "Almen intensity effect on microstructure and mechanical properties of low carbon steel subjected to severe shot peening," *Applied Surface Science*, vol. 290, pp. 40–47, 2014.

[28] N. Kawagoishi, T. Nagano, M. Moriyama, and E. Kondo, "Improvement of fatigue strength of maraging steel by shot peening," *Materials and Manufacturing Processes*, vol. 24, no. 12, pp. 1431–1435, 2009.

[29] R. R. Rego, J. O. Gomes, and A. M. Barros, "The influence on gear surface properties using shot peening with a bimodal media size distribution," *Journal of Materials Processing Technology*, vol. 213, no. 12, pp. 2152–2162, 2013.

[30] S. Bagherifard, I. Fernandez-Pariente, R. Ghelichi, and M. Gugliano, "Effect of severe shot peening on microstructure and fatigue strength of case iron," *International Journal of Fatigue*, vol. 65, pp. 64–70, 2014.

[31] S. M. H. Gangaraj and G. H. Farrahi, "Side effects of shot peening on fatigue crack initiation life," *International Journal of Engineering, Transactions A: Basics*, vol. 24, pp. 275–280, 2011.

[32] K. Zhan, C. H. Jiang, and V. Ji, "Uniformity of residual stress distribution on the surface of S30432 austenitic stainless steel by different shot peening processes," *Materials Letters*, vol. 99, pp. 61–64, 2013.